Morphology of sodium deoxycholate-solubilized apolipoprotein B-100 using negative stain and vitreous ice electron microscopy

Donald L. Gantz,[1] Mary T. Walsh, and Donald M. Small

Department of Biophysics, Boston University School of Medicine, Boston, MA 02118

Abstract **The primary and secondary structures of apolipoprotein B-100 (apoB-100) are well established. Previous morphological studies have suggested that apoB is a long, flexible, threadlike molecule that encircles the low density lipoprotein (LDL) particle. Several large domain regions of the protein have been observed in frozen hydrated LDL and may be involved in anchoring of the protein to the lipid surface of LDL. Calorimetric studies of sodium deoxycholate (NaDC)-solubilized apoB indicated a similar number of independently melting domains. We therefore undertook a morphological study of NaDC-solubilized apoB-100 using negative stain and vitreous ice cryoelectron microscopy, a nonperturbing preservation technique. Negative staining experiments were performed in two ways: *1*) grids were pulled through NaDC-containing buffer surfaces on which monolayers of apoB had been promoted, or *2*) apoB molecules were allowed to diffuse onto carbon surfaces of grids that were floated on sample droplets. Vitrified molecules of apoB were obtained by plunging a thin fluid layer of protein adhered to a holey carbon-coated grid into supercooled ethane and by preserving the molecules in liquid nitrogen. The majority of molecules prepared in negative stain and vitreous ice were curved or arced and had alternating thin and thick regions. In negative stain, the apoB molecules lay on the grid perpendicular to the electron beam and had a mean length of 650 Å. In vitreous ice the molecules were randomly oriented and their images ranged from 160 to 650 Å in length. Vitrified molecules provided visualization of one or two beaded regions. Similar regions were observed in negative stain but the overall thickness was two to three times greater. Some vitrified molecules contained ribbon-like portions. Our study supports previously obtained data on molecule length but suggests that negative staining overestimates molecule width. These first images of vitrified NaDC-solubilized apoB-100 confirm the long, flexible, beaded thread morphology of the molecule and support the unique potential of this technique when coupled with proper molecule orientation and antibody labeling to correlate the tertiary structure of apoB seen in the intact particle with that of the isolated molecule.**—Gantz, D. L., M. T. Walsh, and D. M. Small. **Morphology of sodium deoxycholate-solubilized apolipoprotein B-100 using negative stain and vitreous ice electron microscopy.** ***J. Lipid Res.*** **2000.** 41: **1464–1472.**

Supplementary key words tertiary structure • low density lipoprotein • structural domains

Apolipoprotein B-100 (apoB-100) is a large monomeric glycoprotein of 4,536 amino acids and an approximate molecular weight of 550,000, including carbohydrate (1–3). It is found on low density lipoprotein (LDL) and very low density lipoprotein (VLDL) in human plasma. VLDL and LDL are the major carriers of triglycerides and cholesterol, respectively. High levels of apoB-100 correlate with high levels of apoB-containing lipoproteins, especially LDL, intermediate density lipoprotein (IDL), and VLDL and lead to an increased risk of atherosclerosis. ApoB-100 is synthesized in the liver and assembled with triaclyglycerols, phospholipids, cholesterol, and cholesteryl esters to form nascent VLDL. The nascent VLDL is secreted into plasma and, after a series of exchange and enzymatic reactions, is converted to IDL. Some of the IDL is taken up by the liver and the rest is converted to LDL, which is slowly removed from plasma. Early work using X-ray diffraction and calorimetry (4–8) showed that apoB was on the exterior part of LDL while the lipid core contained cholesteryl esters and triglycerides. Phospholipids were also identified to be exclusively on the surface whereas free cholesterol was distributed between core and surface (5, 8).

In a series of elegant experiments using antibody-decorated, negatively stained LDL, Chatterton et al. (9) showed that apoB encircled the LDL particle with the C-terminal end crossing over itself. The crossing site was identified by Boren et al. (10) to be at amino acids 3500 and 4369. These amino acids, Arg-3500 and Trp-4369, form an association that stabilizes this intersection, preventing the C terminus from blocking the liganding site for the LDL receptor, amino acids 3359–3369. The unique contribution of arginine to this association appears to extend beyond its positive charge and is currently under investigation (10).

In a series of vitreous ice electron microscopy (EM) studies, Spin (11) and Spin and Atkinson (12) showed

Abbreviations: apoB-100, apolipoprotein B-100; CD, circular dichroism; IDL, intermediate density lipoprotein; LDL, low density lipoprotein; NaDC, sodium deoxycholate; VLDL, very low density lipoprotein.

[1] To whom correspondence should be addressed.

apoB to form a belt around the LDL particle with a zigzag at the C terminus. However, in these studies the C terminus appears to lie quite close to the N terminus. These vitreous ice studies requiring no stain show the electron density of the protein, which appears to have several domains. The topology in general corroborates the negative stain work of Chatterton et al. (9, 13).

Little is known about the tertiary structure of apoB-100. Computer modeling of apoB-100 (14, 15) has indicated that there is a globular region at the N terminus followed in turn by large-domain regions rich in β sheet, amphipathic α helix, β sheet, and amphipathic α helix. These five superdomains, perhaps with the exception of the N-terminal globular region, appear to anchor the protein to the lipid surface (16). It has been suggested that the β strand-rich region between apoB-21 and apoB-41, that portion located between the first 21% and the last 59% of the apoB molecule, is an amphipathic β sheet approximately 50 Å wide and 200 Å long (D. M. Small and D. A. Atkinson, unpublished results), and that the entire apoB molecule is approximately 600 to 1,000 Å long and 30 to 100 Å wide (17–19).

The N-terminal 20% of apoB contains seven of the eight disulfide bonds and has a fairly strong homology with lipovitellin and microsomal triglyceride transfer protein (MTP) (20). The lipovitellin structure has been used to model the N-terminal 20% of the apoB sequence. Modeling the first 587 amino acids (the N-terminal 13% of apoB), using the model of vitellogenin obtained from its crystal structure (21), indicates that the first 290 amino acids (~apoB-6) appear to make up a subdomain consisting of an 11-stranded β barrel surrounding a central helix. A second subdomain from amino acids 294 to 587 (B6–B13) is made up of a series of 17 amphipathic helixes. A possible third subdomain of mainly β-sheet structure appears similar to the phospholipid-binding domain of vitellogenin. This N-terminal superdomain appears in the cryoelectron micrographs as an electron-dense globule projecting from the LDL particle, which is clearly marked by antibodies to the N terminus (11, 12).

Walsh and Atkinson (22, 23) showed that apoB can be solubilized in sodium deoxycholate (NaDC) buffer and that it contained both α and β secondary structure. Using high resolution calorimetry they showed that it had five independently melting domains. Because the NaDC-solubilized apoB contains secondary structural characteristics similar to LDL and has calorimetrically defined domains, we have carried out a negative stain and cryoelectron microscopic study of the NaDC-solubilized apoB. Attempts were made to spread and align the molecules at an interface and to bind them to holey grids by pull-through techniques.

The results indicate that apoB is an extended ribbon-like molecule with occasional globular regions, bumps, and a putative loop at one end. We speculate that this loop is located at the C-terminal end.

MATERIALS AND METHODS

Liquid ethane was obtained from Matheson Gas Products (Gloucester, MA) and nitrogen gas from Medical Technology (Medford, MA). Sodium phosphotungstate stain was purchased from Sigma (St. Louis, MO). Sodium deoxycholate (NaDC) was from Calbiochem (La Jolla, CA). Sepharose CL-4B and all chromatographic columns were from Pharmacia-LKB (Piscataway, NJ). Spectrapor dialysis tubing (12–14 and 25 MWCO) was purchased from VWR Scientific (West Chester, PA). Amicon YM-100 ultrafilters and Centricon-100 microconcentrators were from Millipore (Bedford, MA). All electrophoresis chemicals and reagents were from Bio-Rad (Hercules, CA).

Preparation of apoB-100

NaDC-solubilized apoB-100 was prepared from LDL by the method of Walsh and Atkinson (22, 23). Briefly, normal human plasma from a single donor whose LDL contained only the B-100 form of apoB and no other apoproteins was obtained for these studies on multiple occasions. Disodium-EDTA and NaN_3 were added to concentrations of 1 mM and 0.02%, respectively, and LDL of a narrow density range (1.025–1.050 g/ml) was isolated by ultracentrifugal flotation (24), and washed. LDL was dialyzed, the free sulfhydryls of apoB were alkylated, and apoB-100 was solubilized with NaDC and isolated chromatographically as described (22, 23). ApoB-100-containing column fractions were pooled, concentrated to 2 mg/ml by ultrafiltration with Amicon YM100 filters, and dialyzed in Spectrapor dialysis tubing with a 25-kDa cutoff against 50 mM sodium carbonate, 50 mM sodium chloride, 0.02% NaN_3, 10 mM NaDC, pH 10.

Sodium dodecyl sulfate-polyacrylamide gel electrophoresis (SDS-PAGE) analysis of LDL and NaDC-solubilized apoB on 3% tube gels (25) show a single band when stained with Coomassie Brilliant Blue R-250.

Negative stain electron microscopy

Pull-through experiments. ApoB was layered on an aqueous surface and an EM grid was pulled through the surface to achieve an optimum orientation and distribution of apoB-100 molecules. We attempted to produce monolayers of apoB-100 on pH 10.0 buffer (50 mM sodium carbonate, 50 mM sodium chloride, and 0.02% sodium azide) with and without 10 mM NaDC. The protein was originally solubilized in 10 mM NaDC and then diluted 10-fold in nondetergent buffer at a final detergent concentration of 1 mM, which is slightly below its critical micellar concentration (CMC) (26). The procedure was as follows. A 0.3-ml volume of buffer was placed in a well of a clear polystyrene 96-well microtiter assay plate (Corning Costar, Cambridge, MA). A freshly glow-discharged (Balzers Union Glow-Discharge apparatus CTA 010; Bal-Tec Products, Middlebury, CT) 300 mesh carbon, Formvar-coated copper grid (Electron Microscopy Sciences, Fort Washington, PA) held in self-closing forceps (Dumont, Switzerland) was vertically suspended grid down from a plastic clamp attached to a ring stand. The assay plate was placed on the metal platform of a scissor jack ("Big Jack"; Precision Scientific, Chicago, IL), the height of which could be finely controlled. The plate was raised on the jack so that the grid was totally immersed in the well containing the buffer. Next, a 1-μl droplet of a 500-μg/ml suspension of apoB-100 was gently spread on the buffer surface with a 10-μl Hamilton syringe (Hamilton, Reno, NV) and allowed to age for 1 or 30 min. The inside channel of the syringe had previously been coated with apoB-100 in detergent buffer to prevent adherence of the apoB to the glass. The plate buffer well was then lowered slowly (~30 sec) until the grid was no longer in the solution in the buffer well. The grid was immediately negatively stained at pH 10.0 with 1% sodium phosphotungstate, blotted with filter paper, and air dried. The best preparation of molecules of apoB-100 in detergent buffer was obtained when grids were immersed in non-detergent buffer and protein was spread for

1min. However, in general, the pull-through experiments yielded high concentrations of molecules on the grid and few distinct particles for measurement.

Float experiments. A 10-μl droplet of a suspension of apoB-100 at a concentration of 100 μg/ml in pH 10.0 detergent buffer (see above) was placed in a 15 × 60 mm polystyrene petri dish (Becton Dickinson, Lincoln Park, NJ) to minimize evaporation. A freshly glow-discharged (27) carbon, Formvar-coated 300 mesh grid was inverted and floated on the droplet for 0.5, 1, or 5 min, removed, blotted with filter paper, immediately stained with 1% sodium phosphotungstate, pH 10.0, blotted, and air dried. The float experiments yielded a more desirable spread of molecules for measurement.

Vitreous ice cryotransmission electron microscopy

Samples of apoB-100 in detergent buffer (see above) were vitrified (28) by a technique previously described (29). Briefly, a 3-μl aliquot of a suspension of apoB-100 at a concentration of 270 μg/ml in sodium deoxycholate buffer was placed on a freshly glow-discharged holey carbon film (Formvar had been removed) covering a 400 mesh copper grid (Electron Microscopy Sciences). The forceps that held the grid were attached to a nitrogen gas-driven plunger (Charles Ingersoll, Winthrop, PA) in a Plexiglas freezing station (Dan-Kar, Reading, MA). A high humidity environment was maintained around the sample with an ultrasonic humidifier (model TUH-420; Tatung Company of America, Long Beach, CA) and monitored with a humidity meter (Vaisala, Helsinki, Finland). Each sample was blotted from the underside (not sample side) with oven-dried no. 1 filter paper (Whatman Paper, Kent, England) to promote an increase in molecule concentration (30). Fifteen seconds after blotting, each grid was plunged into ethane that had been cooled with liquid nitrogen. Vitrified samples were stored in a cryogenic storage dewar (Taylor-Wharton, Theodore, AL) under liquid nitrogen. For imaging, samples were transferred into a single tilt cryoholder (model 626) using a cryotransfer station (Gatan, Pleasanton, CA) and maintained at 99 K.

Images of negatively stained and vitrified apoB-100 were recorded at a defocus value of 1.4 μ on SO-163 electron image film (Eastman Kodak, Rochester, NY) in a CM-12 transmission electron microscope (Philips Electron Optics, Eindhoven, The Netherlands) equipped with anticontaminator and low dose kit to minimize irradiational damage. The microscope was calibrated with a silicon monoxide grating replica (Ernest F. Fullam, Latham, NY). Micrographs were developed in full-strength D19 (Eastman Kodak) for 12 min.

All particle measurements were made with a Peak ×7 magnifier (Ladd Research Industries, Burlington, VT) with a 1- to 20-mm graticule in 0.1-mm divisions on micrographs enlarged ×2.5 on resin-coated paper. Only distinct molecules with both ends clearly visible were measured. Molecules in clumps or otherwise indistinct were not included. Analysis of images of negatively stained molecules was confined to float experiments because of desirable molecule distributions. Images of negatively stained molecules prepared by the pull-through method were not measured although the general morphology was the same as with the float method. The following data were obtained for each measured molecule: length, width of enlarged regions, if any; minimum and maximum widths of thread portion of molecule, not including enlarged end(s); and the general morphology of the entire molecule (i.e., straight, arc shaped, S shape, circular, horseshoe, hook).

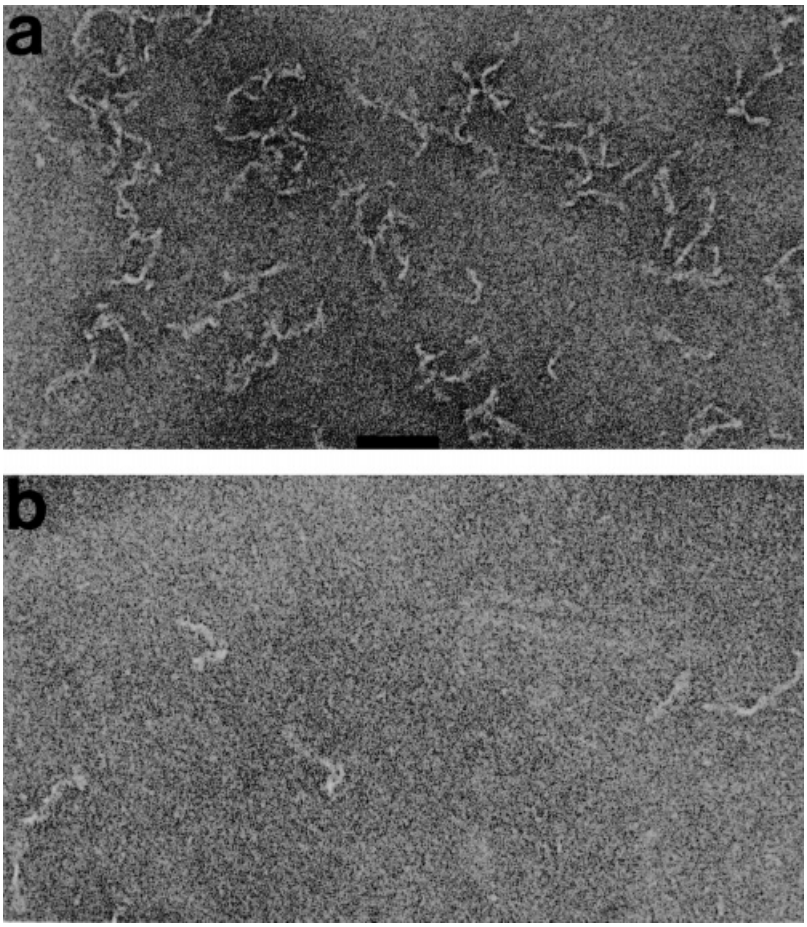

Fig. 1. Distribution of apoB-100 molecules in pH 10 buffer prepared by two different techniques prior to negative staining with 1% sodium phosphotungstate: (a) pull-through technique using apoB-100 at 500 μg/ml with 1 mM NaDC and (b) float technique using apoB-100 at 100 μg/ml with 10 mM NaDC. See Materials and Methods for details. Detergent-solubilized apoB-100 is a long, flexible, threadlike molecule. Bar: 500 Å.

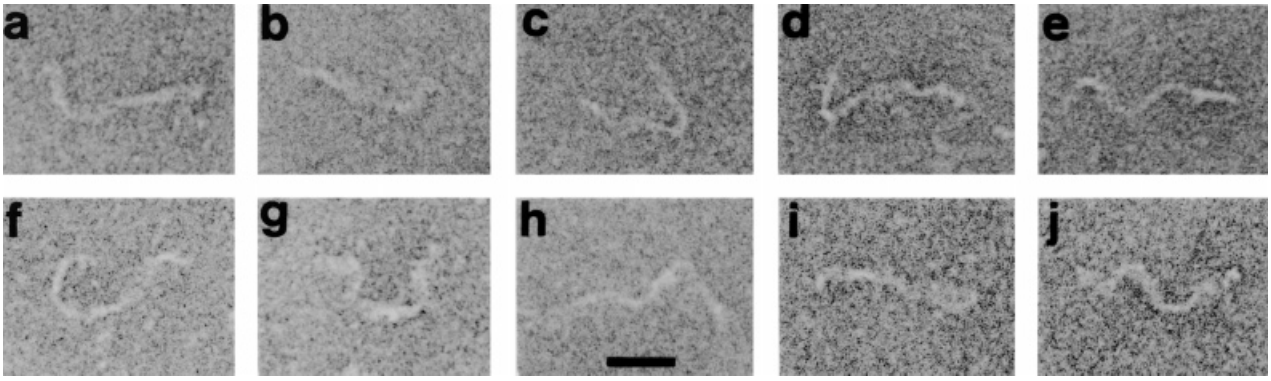

Fig. 2. A gallery of electron micrographs of negatively stained apoB-100 molecules illustrates the variety of morphologies that were commonly observed. (a–e) 500 μg/ml of apoB-100 was prepared in pH 10 buffer containing 1 mM NaDC, using a pull-through technique (see Materials and Methods). Note enlarged end in (e). (f–j) 100 μg/ml of apoB-100 was prepared in pH 10 buffer containing 10 mM NaDC, using a float technique (see Materials and Methods). Note the ribbon-like appearance of the molecule in (g) and two enlarged ends on the molecule in (j). Bar: 250 Å.

RESULTS

ApoB-100/NaDC complexes appear to be long, thin, apparently flexible molecules when negatively stained (**Fig. 1**). The negatively stained images of apoB shown in Fig. 1a and b were the result of pull-through and float experiments, respectively. The molecules present a variety of morphologies, the most common being a curve or arc. A gallery of five enlarged molecules of apoB-100 prepared by the pull-through technique is displayed in **Fig. 2a–e**. All these molecules exhibit a curved or hooked morphology. The molecule in Fig. 2e has a distinctly thicker region at one end. Images of negatively stained molecules prepared in the presence of 10 mM NaDC using the float technique are shown in Fig. 2f–j and illustrate a variety of curved configurations. The molecule in Fig. 2g is unique in that along its length there are two 90° turns and the suggestion of a twisted ribbon morphology. Thickened ends are seen on molecules in Fig. 2g and j.

The electron micrographs in **Fig. 3** show NaDC-solubi-

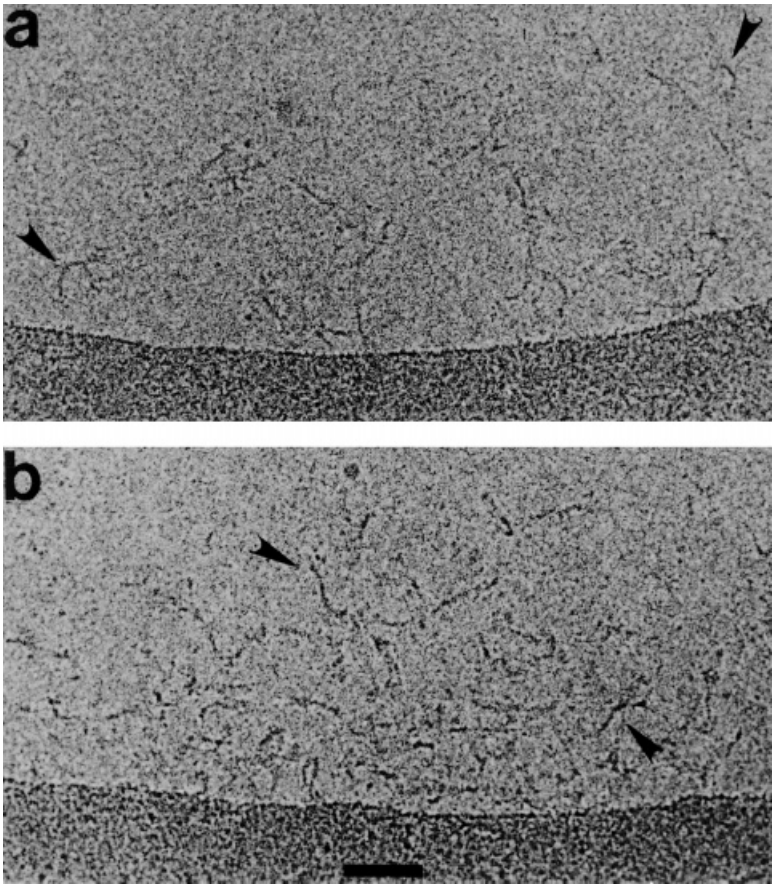

Fig. 3. In vitreous ice, apoB-100 molecules had a beaded-thread appearance, were frequently curved, and were much thinner than in negative stain. Molecules were most distinctive (arrowheads) near edges of holes in thin holey carbon films (carbon edge is at lower portion of micrographs). ApoB-100 was suspended at a concentration of 266 μg/ml in pH 10 buffer containing 10 mM NaDC prior to vitrification. Bar: 500 Å.

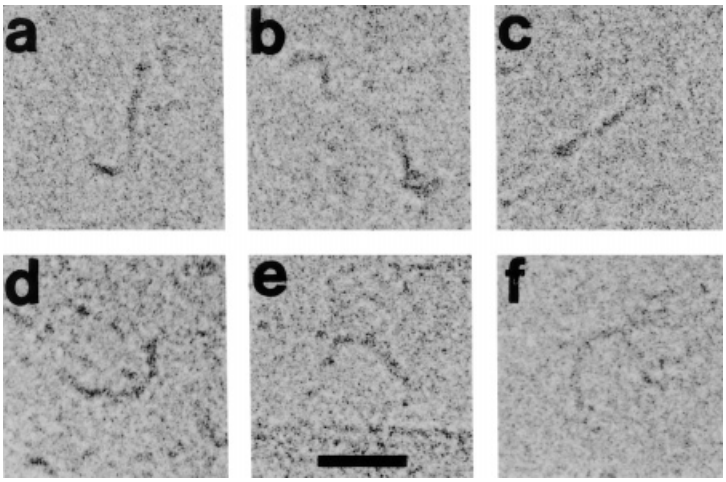

Fig. 4. Six molecules of apoB-100 that were vitrified in pH 10 buffer containing 10 mM NaDC are illustrated in this gallery of electron micrographs. The molecule in (b) has a length similar to the mean length of molecules imaged in negative stain and is probably oriented horizontally in the vitreous ice. Molecules in (a) through (d) each have one beaded end. The molecule in (f) is also seen in Fig. 3a (arrowhead). Bar: 250 Å.

lized apoB molecules embedded in vitreous ice. The molecules are seen as thin strands with slightly enlarged regions of higher density located at various positions along their lengths, particularly at the ends (see arrowheads in Fig. 3a and b). The molecules are assumed to be in random orientation in the vitreous ice layer. In some regions of thicker ice in holes along the carbon edge a superimposition of images occurred and made discrimination of individual molecules difficult. Higher protein dilutions aided in separating particles for measurement.

Six enlarged apoB-100 molecules vitrified in the presence of 10 mM NaDC are presented in **Fig. 4**. Molecules in Fig. 4a–c clearly have enlarged ends. The molecules in Fig. 4b and c and those in Fig. 4d–f illustrate the commonly observed straight and arc-shaped morphologies, respectively. The molecule in Fig. 4B, one of the longest imaged in vitreous ice, has a length of 650 Å, which is similar to the mean length of all measured negatively stained molecules. This molecule is probably oriented horizontally to the plane of the micrograph.

Table 1 compares morphological information of apoB-100 molecules prepared in negative stain and vitreous ice. The distributions of the lengths and widths of molecules in vitreous ice and negative stain are illustrated in **Fig. 5**. The mean length (Å ± SD) of negatively stained molecules was 649 ± 350 Å with a range of 160–2,501 Å (Table 1). Molecules considerably shorter than the mean could be fragments; however, electrophoresis of the isolated protein on

TABLE 1. Comparison of size and morphology of apoB-100 molecules in negative stain and vitreous ice

	Negative Stain[a]	Vitreous Ice[b]
Length[c] (Å)		
Mean	649 ± 350	342 ± 120
Median	552	320
Range	160–2501 (n = 305)	160–650 (n = 55)
Width of threads[d] (Å)		
Mean	57 ± 18	21 ± 7
Median	53	18
Range	18–151 (n = 305)	13–45 (n = 55)
Width of enlarged ends[e] (Å)		
Mean	104 ± 35	37 ± 15
Median	98	36
Range	45–249 (n = 157)	18–71 (n = 36)
Morphology[f] (%)		
Arc	45	33
Straight	37	40
S shaped	9	4
Circular	2	0
Horseshoe	4	18
Hook	3	5

[a] Data are from molecules prepared in float experiments in the presence of 10 mM NaDC. See Materials and Methods. Examples appear in Fig. 1b and 2f–j. Data were derived from 25 micrographs and 2 grids.
[b] Molecules were vitrified in the presence of 10 mM NaDC. See Materials and Methods. Examples appear in Fig. 3a and b and Fig. 4a–f. Data were derived from nine micrographs and one grid.
[c] Entire length of molecule includes threaded portion and enlarged ends.
[d] Minimum and maximum widths of threaded portion of each molecule were averaged.
[e] In negative stain, 41% of molecules had one enlarged end, 11% had two. In vitreous ice, 51% of molecules had one enlarged end, 15% had two.
[f] Each molecule was assigned to a morphological category. Data in each column represent percent of total.

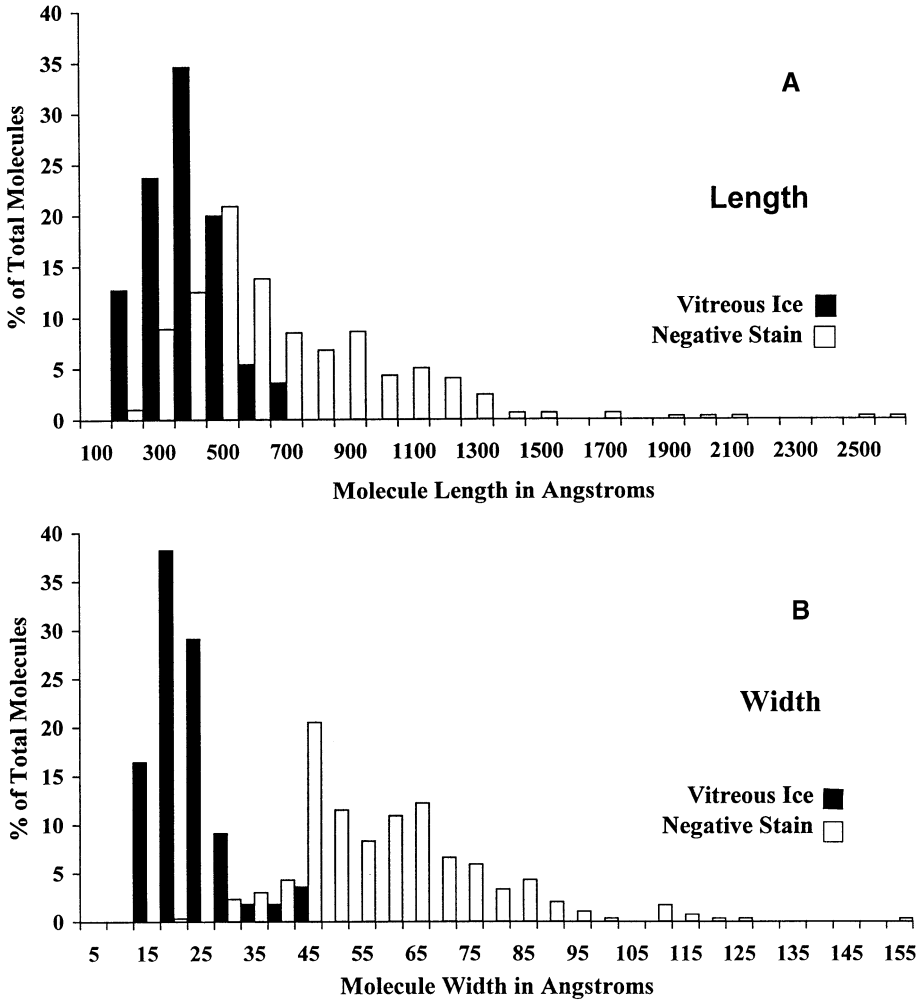

Fig. 5. Histograms of lengths (A) and widths (B) of apoB-100 molecules in vitreous ice and negative stain illustrate the difference in size ranges obtained with the two techniques. In histogram (A) the medians and means of molecule lengths in ice and negative stain were as follows: 320 and 342 Å, and 552 and 649 Å, respectively. In (B), the medians and means of molecule widths were 18 and 21 Å, and 53 and 57 Å, respectively. All molecules were prepared in the presence of 10 nM NaDC.

3% gels indicated negligible degradation (data not shown). Molecules much longer than the mean may be dimers or trimers associated roughly end-to-end. In vitreous ice, the mean length (Å ± SD) of the molecules was 342 ± 120 Å with a range of lengths of 160–650 Å. The lower mean length of molecules in vitreous ice compared with negative staining is due to the random orientation of the molecules in the ice layer; most molecules are probably not parallel to the plane of ice. The length of the longest molecule seen in vitreous ice is similar to the average length of molecules observed in negative stain. The fact that no molecules longer than 650 Å were seen in ice clearly suggests that images greater than ~700 Å were formed in negative stain by association of more than one apoB molecule.

The averaged values for the widths of the threaded portions of the molecules are shown in Table 1. The mean width (Å ± SD) of molecules in vitreous ice was 21 ± 7 Å and the range was 13–45 Å. The mean width of molecules in negative stain was 2.5 to 3 times larger than that in vitreous ice.

Beaded or enlarged regions, possible structural domains, were observed in some molecules in both negative stain and vitreous ice (Figs. 2 and 4). Some molecules contained one enlarged end (Fig. 2e and Fig. 4a and b) or two enlarged ends (Fig. 2j). Some molecules did not have obvious beaded regions (Fig. 2a, b, and d and Fig. 4d and e). In negative stain, 41% of the molecules had one enlarged end and 11% had two. Among 55 molecules in vitreous ice, 27 had no distinct beads, 28 (51%) had at least one bead, and 7 (11%) had two.

The morphological heterogeneity of these molecules prepared in negative stain and vitreous ice suggests an inherent flexibility to the molecule. In each of these two microscopy techniques, approximately 60% of the molecules were arclike, hooked, or curved (Table 1). Interpretation of the shapes of molecules in vitreous ice should be made cautiously, however, because orientation of molecules in the thicker ice layers at hole edges is random.

The shapes of the enlarged regions in molecules that were negatively stained were variable: round, ovoid, trian-

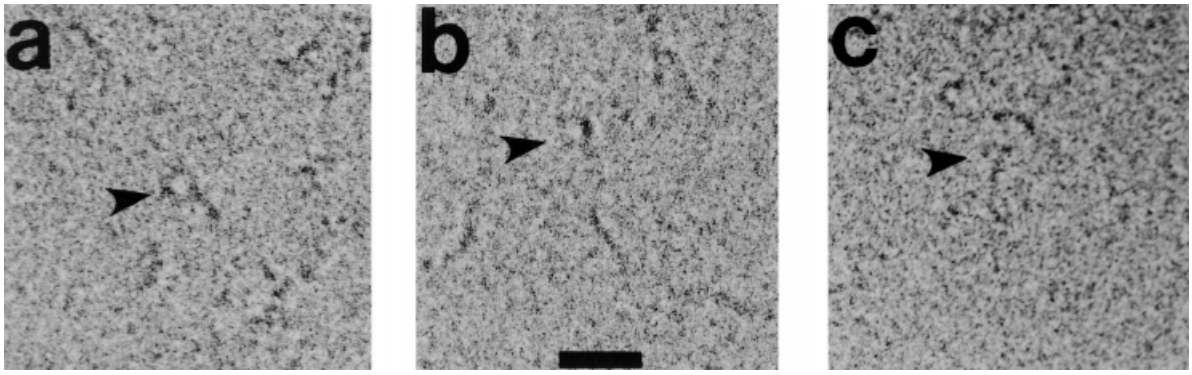

Fig. 6. These electron micrographs of vitrified apoB-100 molecules suggest the presence of a loop at one end (arrowheads). Loops are proposed to be at the carboxy-terminal end of the apoB molecule in the intact LDL particle (10). ApoB-100 had been solubilized in pH 10 buffer containing 10 mM NaDC. Bar: 250 Å.

gular (Fig. 2e and j), and forked (Fig. 2f). On the other hand, the beaded portions of molecules in vitreous ice were generally round to ovoid (Fig. 4a–c).

In the thread portion of some molecules (between beaded regions), broader ribbon-like segments were observed in both negative stain and vitreous ice (Fig. 2f, g, and j and Fig. 4b). The middle portion of the molecule in vitreous ice (Fig. 4b) was less dense and slightly wider.

Occasionally, a small loop at one end of a molecule was observed. Three images of apoB-100 molecules embedded in vitreous ice are presented in **Fig. 6** to illustrate the loops. The looped molecule in Fig. 6a may be oriented almost perpendicular to the plane of the micrograph while those molecules in Fig. 6b and c are oriented closer to the horizontal plane.

DISCUSSION

The size and morphological information that we have obtained from negatively stained images of NaDC-solubilized apoB-100 (Table 1) is similar to that obtained by others who have studied this molecule in a variety of detergents, using several different electron microscopy techniques but not vitreous ice cryoelectron microscopy (17–19). In a study by Zampighi, Reynolds, and Watt (17) apoB-100 obtained from fasting human LDL was solubilized with *n*-dodecyl octaethyleneglycol monoether and shadow casted with platinum/carbon at angles of 10 to 30°. This protein-detergent complex appeared as a flexible rod (assuming various curved shapes, including a horseshoe) that was 750–800 Å long and 45–55 Å wide. The molecules had a tendency to associate in a lateral fashion (17). In a study by Ikai (18) a negatively stained apoB-Tween 80 complex appeared as a highly asymmetric flexible string of 1,000 Å in length and 50–60 Å in width that assumed many conformations. In a third study, the morphology of apoLDL$_2$, solubilized in sodium deoxycholate and analyzed by freeze fracture and freeze etching (19), was elongated and flexible with an asymmetric distribution peaking at 75 Å and extending to two or three times this length. In contrast, the morphology of water-soluble apoB was globular (31). In this work the apoB from human LDL obtained after a 12-h fast, was reduced and carboxymethylated, and then diluted with 1% ammonium acetate. Negatively stained and freeze-fractured preparations showed a globular-shaped protein with mean diameters of 115 and 130 Å, respectively (31).

The negative stain and shadowing techniques are useful in determining the length of the apoB-100 molecule because of the fixed horizontal orientation of the molecules on the grid. However, these techniques clearly have overestimated the width of the molecule based on data that we have obtained by vitreous ice cryomicroscopy, a technique that should preserve the molecules close to their original state in suspension. The widths of the molecules in negative stain are 2- to 3-fold higher than those in vitreous ice (Table 1, Fig. 5). The overestimation of width is likely caused by flattening of the molecule on absorption to the carbon surface on the grid prior to negative staining or shadowing. On the other hand, the lengths of apoB-100 molecules in vitreous ice are underestimated because of the random orientation of the molecules (Table 1, Fig. 5).

We frequently observed one or two enlarged or beaded regions at the ends of molecules prepared in negative stain and vitreous ice (Table 1). The enlarged ends in negatively stained molecules were larger and more heterogeneous in shape than in vitrified molecules. This difference could be caused by flattening and perturbation of the ends when absorbed to the carbon surface prior to staining. The beads in molecules embedded in vitreous ice were typically ovoid in shape. The vitreous ice cryomicroscopy technique may be useful in determining the number and position of globular domains along isolated protein molecules for comparison with those domains already observed in the intact LDL particle (12), particularly if orientation of the molecules in vitreous ice can be restricted to the horizontal plane. The number and position of domains in the isolated protein may not correspond to the four or five domains or superdomains of apoB observed in the intact LDL particle (12). Although sodium deoxycholate-solubilized apoB-100 retained a secondary conformation similar to that of the protein in LDL and to the protein associated with NaDC mixed micelles (22) as

analyzed by far-UV circular dichroism (CD), the tertiary structure of apoB-100 in LDL and in NaDC was shown to be different on the basis of near-UV CD studies (23). The binding of a monoclonal antibody specific for the N terminus of apoB in intact LDL to the N-terminal end of the apoB molecule would aid in identification of the orientation. Such studies are currently in progress.

Several studies of apoB in intact LDL have indicated that the protein is distributed at the lipid-water interface in LDL and contains dense regions that are probably domains. The mapping of apoB-100 on the surface of LDL by triangulation techniques with six monoclonal antibodies generated the idea that the protein is a belt wrapping once around the LDL particle with the C terminal crossing back over itself near the LDL receptor liganding region (9, 13). Boren et al. (10) have identified the crossing site at Arg-3500 and Trp-4369 where these two amino acids form a bond. Because the ligand-binding site for the LDL receptor on apoB is at amino acids 3359–3369, it is free to bind to the LDL receptor as long as the chain is bound at Arg-3500. In familial dysbetalipoproteinemia (R3500Q) binding is broken and the carboxy-terminal portion apparently hinders binding of region 3359–3369 to the LDL receptor. Using cryoelectron microscopy to observe human LDL in vitreous ice, projections of the peripheral dense ring in LDL believed to be apoB-100 indicated four or five large regions of high electron density that are probably protein superdomains (12). In another study, images of frozen, hydrated human LDL produced two different particle projections: *1*) round with a dense peripheral ring, which suggested one protein molecule, and *2*) discoidal with two parallel high density bands suggesting a double ring of protein (32). This discoidal or rectangular morphology of LDL was also observed by Spin and Atkinson (12) and was considered to be caused by the oxidation of LDL prior to vitrification. In addition, negatively stained images of LDL that had been absorbed to a carbon-coated grid and then extracted with ethanol-ether revealed circular structures of length 600–700 Å containing multiple domains of width 20–70 Å (33).

That the apoB molecule has an inherent flexibility seems to be generally accepted in studies of apoB–detergent complexes and in the intact LDL particle (9, 13, 17–19). We also observed this flexibility in both negative stain and vitreous ice images. In fact, when the morphologies of molecules prepared by these two techniques were compared (Table 1), the percentages of curved (60%) versus straight (40%) molecules were remarkably similar. We would expect that the random orientation of molecules in vitreous ice would allow some curved molecules to appear straight. Curved molecules suspended in detergent might not remain curved when prepared in negative stain because of surface interactions with the negatively charged, hydrophilic carbon surface on absorption and drying.

According to a model of the intact LDL particle proposed by Boren et al. (10), a loop is created where the carboxy-terminal tail crosses the apoB-100 molecule. The loop is stabilized by the binding of Arg-3500 to Trp-4369 and could serve to modulate binding to the LDL receptor. Approximately 20% of the total 4,536 amino acids in apoB-100 are part of this loop. It is not known whether these loops are preserved in NaDC-solubilized apoB-100. A few loops were seen in images of molecules prepared in negative stain and vitreous ice. Some of the loops in negatively stained molecules contained almost 40% of the total molecule length and are probably an artifact of the technique. Artifactually formed loops are less likely in vitrified molecules but in only a small proportion of vitrified molecules could we identify loops (Fig. 6). The size of these loops correlates with the dimensions of the C-terminal loop proposed by Boren et al. (10), but until they can be marked by C-terminal antibodies we can only speculate concerning their identity.

We thank Dr. David Atkinson for critical reading of the manuscript. We thank Mr. Michael Gigliotti for the isolation of LDL. We are indebted to Ms. Donna Ross for assistance in preparation of the manuscript. Our work was supported by NIH Grant P01-HL26335.

Manuscript received 12 October 1999 and in revised form 19 May 2000.

REFERENCES

1. Knott, T. J., R. J. Pease, L. M. Powell, S. C. Wallis, S. C. Rall, Jr., T. L. Innerarity, B. Blackhart, W. H. Taylor, Y. Marcel, R. Milne, D. Johnson, M. Fuller, A. J. Lusis, B. J. McCarthy, R. W. Mahley, B. Levy-Wilson, and J. Scott. 1986. Complete protein sequence and identification of structural domains of human apolipoprotein B. *Nature.* **323:** 734–738.
2. Yang, C-Y., S-H. Chen, S. H. Gianturco, W. A. Bradley, J. T. Sparrow, M. Tanimura, W-H. Li, D. A. Sparrow, H. DeLoof, M. Rosseneu, F-S. Lee, Z-W. Gu, A. M. Gotto, Jr., and L. Chan. 1986. Sequence, structure, receptor-binding domains and internal repeats of human apolipoprotein B-100. *Nature.* **323:** 738–742.
3. Cladaras, C., M. Hadzopoulou-Cladaras, R. T. Nolte, D. Atkinson, and V. I. Zannis. 1986. The complete sequence and structural analysis of human apolipoprotein B-100: relationship between apoB-100 and apoB-48 forms. *EMBO J.* **5:** 3495–3507.
4. Deckelbaum, R. J., G. G. Shipley, D. M. Small, R. S. Lees, and P. K. George. 1975. Thermal transitions in human plasma low density lipoproteins. *Science.* **190:** 392–394.
5. Deckelbaum, R. J., G. G. Shipley, and D. M. Small. 1977. Structure and interactions of lipids in human plasma low density lipoproteins. *J. Biol. Chem.* **252:** 744–754.
6. Laggner, P., K. Müller, O. Kratky, G. Kostner, and A. Holasek. 1976. X-ray small angle scattering on human plasma lipoproteins. *J. Colloid Interface Sci.* **55:** 102–108.
7. Atkinson, D., R. J. Deckelbaum, D. M. Small, and G. G. Shipley. 1977. Structure of human plasma low-density lipoproteins: molecular organization of the central core. *Proc. Natl. Acad. Sci. USA.* **74:** 1042–1046.
8. Müller, K., and P. Laggner. 1978. The structure of human-plasma low-density lipoprotein B: an X-ray small-angle scattering study. *Eur. J. Biochem.* **82:** 73–90.
9. Chatterton, J. E., M. L. Phillips, L. K. Curtiss, R. Milne, J-C. Fruchart, and V. N. Schumaker. 1995. Immunoelectron microscopy of low density lipoproteins yields a ribbon and bow model for the conformation of apolipoprotein B on the lipoprotein surface. *J. Lipid Res.* **36:** 2027–2037.
10. Boren, J., I. Lee, W. Zhu, K. Arnold, S. Taylor, and T. L. Innerarity. 1998. Identification of the low density lipoprotein receptor-binding site in apolipoprotein B100 and the modulation of its binding activity by the carboxyl terminus in familial defective apo-B100. *J. Clin. Invest.* **101:** 1084–1093.
11. Spin, J. M. 1997. Cryoelectron Microscopy Studies of Low Density Lipoprotein in Vitreous Ice. PhD Thesis. Boston University School of Medicine, Boston, MA. 289 (University Microfilms, Inc., 97–13151).

12. Spin, J. M., and D. Atkinson. 1995. Cryoelectron microscopy of low density lipoprotein in vitreous ice. *Biophys. J.* **68:** 2115–2123.
13. Chatterton, J. E., M. L. Phillips, L. K. Curtiss, R. W. Milne, Y. L. Marcel, and V. N. Schumaker. 1991. Mapping apolipoprotein B on the low density lipoprotein surface by immunoelectron microscopy. *J. Biol. Chem.* **266:** 5955–5962.
14. Nolte, R. T. 1994. Structural Analysis of the Human Apolipoproteins: An Integrated Approach Utilizing Physical and Computational Methods. Vols. I and II. PhD Thesis. Boston University School of Medicine, Boston, MA (University Microfilms, Inc., 93–32587).
15. Segrest, J. P., M. K. Jones, V. K. Mishra, G. M. Anantharamaiah, and D. W. Garber. 1994. ApoB-100 has a pentapartite structure composed of three amphipathic α-helical domains alternating with two amphipathic β-strand domains. *Arterioscler. Thromb.* **14:** 1674–1685.
16. Yang, C-Y., Z-W. Gu, S-A. Weng, T. W. Kim, S-H. Chen, H. J. Pownall, P. M. Sharp, S-W. Liu, W-H. Li, A. M. Gotto, Jr., and L. Chan. 1989. Structure of apolipoprotein B-100 of human low density lipoproteins. *Arteriosclerosis.* **9:** 96–108.
17. Zampighi, G., J. A. Reynolds, and R. M. Watt. 1980. Characterization of apolipoprotein B from human serum low density lipoprotein in *n*-dodecyl octaethyleneglycol monoether: an electron microscope study. *J. Cell Biol.* **87:** 555–561.
18. Ikai, A. 1980. Extraction of the apo B cluster from human low density lipoprotein with Tween 80. *J. Biochem.* **88:** 1349–1357.
19. Gulik, A., L. P. Aggerbeck, J. C. Dedieu, and T. Gulik-Krzywicki. 1982. Freeze-fracture electron microscopic analysis of solutions of biological molecules. *J. Microsc.* **125:** 207–213.
20. Anderson, T. A., D. G. Levitt, and L. J. Banaszak. 1998. The structural basis of lipid interactions in lipovitellin, a soluble lipoprotein. *Structure.* **6:** 895–909.
21. Mann, C. J., T. A. Anderson, J. Read, S. A. Chester, G. B. Harrison, S. Köchl, P. J. Ritchie, P. Bradbury, F. S. Hussain, J. Amey, B. Vanloo, M. Rosseneu, R. Infante, J. M. Hancock, D. G. Levitt, L. J. Banaszak, J. Scott, and C. C. Shoulders. 1999. The structure of vitellogenin provides a molecular model for the assembly and secretion of atherogenic lipoproteins. *J. Mol. Biol.* **285:** 391–408.
22. Walsh, M. T., and D. Atkinson. 1983. Solubilization of low-density lipoprotein with sodium deoxycholate and recombination of apoprotein B with dimyristoylphosphatidylcholine. *Biochemistry.* **22:** 3170–3178.
23. Walsh, M. T., and D. Atkinson. 1990. Calorimetric and spectroscopic investigation of the unfolding of human apolipoprotein B. *J. Lipid Res.* **31:** 1051–1062.
24. Havel, R. J., H. A. Eder, and J. H. Bragdon. 1955. Distribution and chemical composition of ultracentrifugally separated lipoproteins in human serum. *J. Clin. Invest.* **34:** 1345–1353.
25. Weber, K., and M. J. Osborn. 1969. The reliability of molecular weight determinations by dodecyl sulfate-polyacrylamide gel electrophoresis. *J. Biol. Chem.* **244:** 4406–4412.
26. Cabral, D. J., and D. M. Small. 1989. The physical chemistry of bile. *In* Handbook of Physiology: The Gastrointestinal System III. S. G. Schultz, J. G. Forte, and B. B. Rauner, editors. American Physiological Society, Waverly Press, Baltimore, MD. 621–662.
27. Dubochet, J., M. Groom, and S. Mueller-Neuteboom. 1982. The mounting of macromolecules for electron microscopy with particular reference to surface phenomena and the treatment of support films by glow discharge. *Adv. Opt. Electron Micros.* **8:** 107–135.
28. Dubochet, J., M. Adrian, J. J. Chang, J. C. Homo, J. Lepault, A. W. McDowell, and P. Schultz. 1988. Cryo-electron microscopy of vitrified specimens. *Q. Rev. Biophys.* **21:** 129–228.
29. Gantz, D. L., D. Q-H. Wang, M. C. Carey, and D. M. Small. 1999. Cryo-electron microscopy of a nucleating model bile in vitreous ice: formation of primordial vesicles. *Biophys. J.* **76:** 1436–1451.
30. Toyoshima, C. 1989. On the use of holey grids in electron crystallography. *Ultramicroscopy.* **30:** 439–444.
31. Lee, D. M., D. L. Stiers, and T. Mok. 1987. Apolipoprotein B is a globular protein—morphological studies by electron microscopy. *Biochem. Biophys. Res. Commun.* **144:** 210–216.
32. Van Antwerpen, R., and J. C. Gilkey. 1994. Cryo-electron microscopy reveals human low density lipoprotein substructure. *J. Lipid Res.* **35:** 2223–2231.
33. Phillips, M. L., and V. N. Schumaker. 1989. Conformation of apolipoprotein B after lipid extraction of low density lipoproteins attached to an electron microscope grid. *J. Lipid Res.* **30:** 415–422.